

Modeling of ring resonators as optical Filters using MEEP

I. M. Matere , D. W. Waswa , J Tonui and D. Kiboi Boiyo

Abstract— Ring Resonators are key component in modern optical networks. Their size allows high density integration in optical photonic circuits due to the use of high index contrast. Ring Resonators based filters in wavelength division multiplexing are considered as one example in this technology. In this study, we theoretically demonstrate Ring resonators for optical filter applications. Coupling a closed loop resonator with a straight waveguide using evanescent coupling, leads to a filter behavior of a new structure. By using Mit Electromagnetic Equation Propagation (MEEP) the transfer functions, resonance frequency of 1.45×10^{15} rad/s, resonance wavelength of $1.2955 \mu\text{m}$ and characteristics of a tunable optical filter showed a good agreement between analytical and simulation based results. This work is of great interest in designing add/drop in wavelength division multiplexing (WDM) which will improve the selection of the optical signal and data fibre to home (FTH).

Keywords— Free spectral Range (FSR), Finesse (F), Quality factor (Q) and Tunable filter.

I. INTRODUCTION

The fundamental building blocks of Ring resonators based devices are a micro-ring with one or two waveguides [1]. In the former case this leads to two-port devices, which act as all-pass filter. On the other hand, a Ring Resonator consisting of a ring with two straight waveguides represents a 4-port structure in photonic integrated circuits which are the next generation of optical networks where the optical components are of small size and high density. High refractive contrast waveguides represent good candidates for future optical circuits. Optical ring resonators are used in circuits as all-pass filters, add/drop filters and biosensors [2] [3]. A waveguide with a perimeter of several micrometers is used to construct an optical resonators, this ring supports a number of circulating wavelengths that satisfy the resonant condition [4].

$$\theta + \varphi_t = 2\pi m \quad (1)$$

where φ_t is the phase of the coupler, m is an integer representing the mode number and $\theta = \omega L/c$, L is the circumference of the ring, given by $L = 2\pi r$, r being

I. M. Matere, D. W. Waswa and J. Tonui Department of Physics, University of Eldoret: +2540720886040; fax: +254532063257; Correspondent e-mail: matereisaac@yahoo.com

D. Kiboi Boiyo, Centre for Broadband Communications, Nelson Mandela Metropolitan University, Port Elizabeth, South Africa

the radius of the ring measured from the center of the ring to the center of the waveguide, c is the phase velocity of the ring mode [5] $c = c_0/n_{eff}$. The fixed angular frequency, $\omega = kc_0$, c_0 refers to the vacuum speed of light. The vacuum wavenumber k is related to the wavenumber λ through: $k = 2\pi/\lambda$. Free spectral range (FSR) is the difference between two resonance wavelengths which is of interest in wavelength division multiplexing (WDM). The resonator is then coupled to an external circuit to get the transfer of stored energy. This is achieved by using a single or a double straight waveguides close to the ring. The coupling between the evanescent modes of the ring and the waveguide produces a transfer of stored energy in the ring to the output port of the waveguide [6] [7]. A small size ring resonator are modeled using, Gallium Indium Arsenide Phosphide (GaInAsP) which offers a high index contrast between core and cladding to ensure a high confinement of light and hence reducing the bending losses. [8]. In WDM the free spectral range is required to be as high as possible (30 nm) [9] in the C-window and around 1550 nm [10], this implies that using a small radius in the range of $5 \mu\text{m}$, but reducing the radius of the ring will result in increasing of bending loss to unacceptable levels. However using rings of varied radii coupled with each other to two outer straight waveguides represents an alternative for increasing FSR [11].

II. METHODOLOGY

2.0 Ring Resonator Transfer Functions

The tested ring had a core radius of R_C and a thickness of $1 \mu\text{m}$, meaning that as the radius is increased their will be an addition of the thickness of the ring. In this case $R_1 = R_C$ and $R_2 = R_C + 1 \mu\text{m}$. The refractive index of the ring is $n=3.4$ which is a high refractive index contrast;

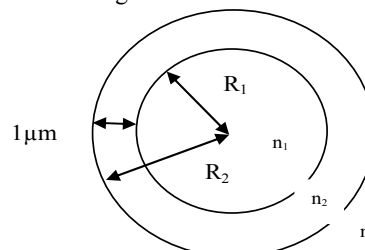


Fig 1: A ring with radii R_1 and R_2 with refractive indices increasing from the centre.

The transfer function is affected by the characteristics of coupling regions represented by the power coupling coefficients t and through coefficients k with t^* and k^* as their conjugate. For lossless coupling;

$$(2) \quad |k^2 + |t^2| = 1|$$

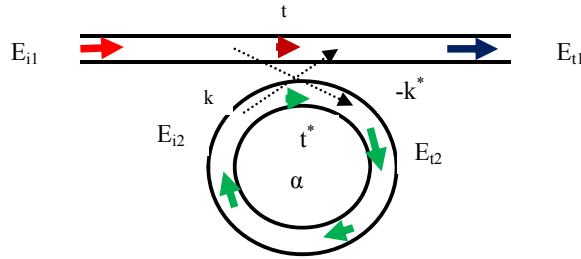


Fig 2: Model of a single ring resonator with one waveguide

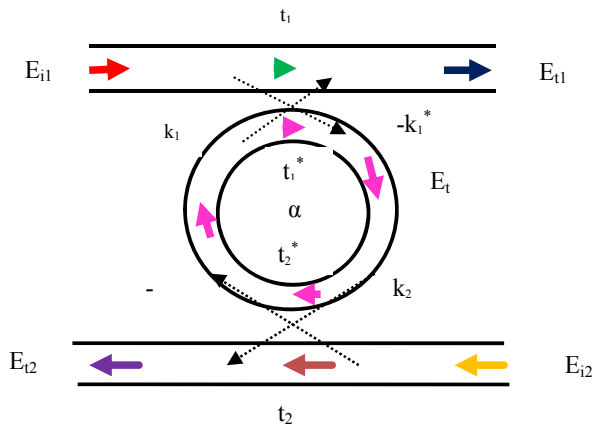


Fig 3: Model of a single ring resonator with two waveguide

For a single unidirectional mode of the resonator, the coupling is lossless so single polarization is considered implying that the various kinds of losses occurring along the propagation of light in the ring resonator filter are incorporated in the attenuation constant represented by the matrix [12].

$$(3) \quad \begin{pmatrix} E_{t1} \\ E_{t2} \end{pmatrix} = \begin{pmatrix} t & k \\ -k^* & t^* \end{pmatrix} \begin{pmatrix} E_{i1} \\ E_{i2} \end{pmatrix}$$

For further simplification the modal E_{i1} is chosen to be 1. Then the round trip in the ring will be $E_{i2} = \alpha \cdot e^{j\theta} E_{t2}$. The resonance condition will be the round trip phase shift a multiple of 2π . The phase shift is a function of wavelength, propagation constant and the length of the resonator;

$$\beta = k \cdot n_{eff} = \frac{2\pi \cdot n_{eff}}{\lambda}$$

(4)

where β is the propagation constant which is a function of wavelength and structure specification represented by effective refractive index. The complex mode amplitudes E are normalized so that their squared magnitude corresponds to the modal power.

$$E_{t1} = \frac{-\alpha + t \cdot e^{-j\theta}}{-\alpha t^* + e^{-j\theta}} \quad (5)$$

where α is the circulating loss factor of the ring

$$E_{i2} = \frac{-\alpha k^*}{-\alpha t^* + e^{-j\theta}} \quad (6)$$

The power transfer characteristics are described by

$$P_{t1} = \left| \frac{E_{t1}}{E_{i1}} \right|^2 = |E_{t1}|^2 = \frac{(\alpha - |t|)^2}{(1 - \alpha|t|)^2} \quad (7)$$

The circulating power P_{i2} is given by

$$P_{i2} = |E_{i2}|^2 = \frac{\alpha^2(1 - |t|^2)}{(1 - \alpha|t|)^2} \quad (8)$$

Two features of equation (8) illustrate most of potential applications; (1) there exists a special condition, ($\alpha = |t|$) when the internal losses ($1 - \alpha^2$) are equal to the coupling losses ($1 - |t|^2$) for which the transmitted power is zero, (2) at ($\alpha > |t|$) the transmission is much higher. It is apparent that in high-Q resonators ($\alpha \approx 1$), small modulation of α or t , causes large modulation of the transmitted power. This can be used to construct electro-optic modulators. In addition to the undercoupled region ($\alpha < t$), as the gain is increased, the power transmission decreases until the critical coupling point ($\alpha = 1$) [13].

From equation (1) to (8), it is possible to get a good idea of the behaviour of a simplified basic ring resonator filter configuration consisting of only one waveguide and a ring.

An addition of a second waveguide leads to the following amplitude mode power output from the drop port as in Fig 2. The throughput port (E_{t1}) mode amplitude in the first waveguide is given by[14];

$$E_{t1} = t_1 + \frac{-k_1 k_1^* t_2^* \alpha_{1/2}^2 e^{j\theta} |t_1|^2 + |k_1|^2 = 1}{1 - t_1^* t_2^* \alpha_{1/2}^2 e^{j\theta}}$$

III. RESULTS AND DISCUSSIONS

$$\begin{aligned} &= \frac{t_1 - t_2^* \alpha_{1/2}^2 e^{j\theta}}{1 - t_1^* t_2^* \alpha_{1/2}^2 e^{j\theta}} \\ &= \frac{t_1 - t_2^* \alpha e^{j\theta}}{1 - t_1^* t_2^* \alpha e^{j\theta}} \end{aligned} \quad (9)$$

The mode amplitude in the ring has to pass the second coupler to become the new dropped mode amplitude E_{t2} . This mode is given by;

$$E_{t2} = \frac{-k_1^* k_2 \alpha_{1/2} e^{j\theta_{1/2}}}{1 - t_1^* t_2^* \alpha e^{j\theta}} \quad (10)$$

During resonance $(\theta + \varphi_t) = 2\pi m$ the output power from the drop port will be;

$$\begin{aligned} P_{t2-Resonance} &= |E_{t2-Resonance}|^2 \\ &= \frac{(1 - |t|)^2 \cdot (1 - |t_2|^2) \cdot \alpha}{(1 - \alpha |t_1 t_2|)^2} \end{aligned} \quad (11)$$

2.1 Free Spectral Range (FSR)

This is the difference in position between two consecutive resonant peaks and can be defined either in frequency or wavelength domain (FSR_f or FSR_λ) respectively.

$$FSR_f = \Delta f = \frac{c_0}{n_g 2\pi R}, FSR_\lambda = \Delta \lambda \approx \frac{\lambda^2}{n_g 2\pi R} \quad (12)$$

R is the radius of the ring, n_g is the group refractive index and $\Delta f, \Delta \lambda$ is the difference in position between two consecutive resonant peaks frequency and wavelength respectively.

2.2 Finesse F

This is the ratio of the FSR and Full Width at Half Maximum (FWHM) [14].

$$\begin{aligned} F &= \frac{FSR}{FWHM} \\ &= \frac{\Delta \lambda}{2 \delta \lambda} \end{aligned} \quad (13)$$

2.3 Quality factor Q

This is the measure of the sharpness of the resonance. It is defined as the ratio of the operation wavelength and the resonance width.

$$\begin{aligned} Q &= \frac{\lambda}{2 \delta \lambda} = \pi \frac{n_{eff} L}{\lambda} \frac{t}{1 - t^2} \\ &= \frac{n_{eff} L}{\lambda} F \end{aligned} \quad (14)$$

3.0 Resonant modes

The tested structures had radii of between $R_C = 5 \mu m$ and $R_C = 200 \mu m$ from which the resonance wavelength which results in a real angular frequency of $1.45 \times 10^{15} \text{ rad/s}$ was $1.2955 \mu m$ was achieved. The summary of the calculated resonant modes are shown in table I and II.

Table I: calculated resonant wavelength of a Ring Resonator

Radius R [μm]	$\lambda_{res} [\mu m]$ [15]	$\lambda_{res} [\mu m]$ (MEEP calculation)
5	1.29192	1.285
10	1.29513	1.278
20	1.29763	1.277
30	1.29859	1.301
40	1.29819	1.297
50	1.29965	1.287
60	1.30006	1.314
80	1.30074	1.299
100	1.29965	1.316
200	1.30008	1.301

Table II: calculated resonant frequency of a Ring Resonator

Radius R [μm]	$Re(\omega) \times$ 10^{15} rad/s [15]	$Re(\omega) \times 10^{15} \text{ rad/s}$ (MEEP calculations)
5	1.4590	1.4664
10	1.4554	1.4753
20	1.4526	1.4766
30	1.4515	1.4493
40	1.4509	1.4531
50	1.4504	1.4646
60	1.4499	1.4343
80	1.4491	1.4509
100	1.4504	1.4327
200	1.4499	1.4486

3.1 Two waveguides with a ring

The power that is transmitted from the input to the output of the Ring resonator maximum near the ring than in other regions as shown in Fig 5

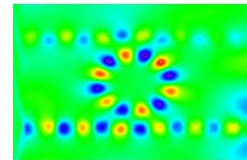


Fig 4: Ring resonator in transmission

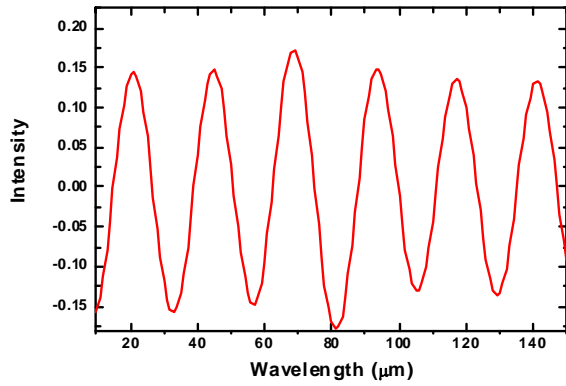


Fig 5: Power transmission in the ring resonator with amplitude

The power coupled in the ring in Fig 2 above is high at resonance other than other parts of the waveguide because the ring and the port waveguides are evanescently coupled and a fraction of the incoming field is transferred to the ring. When the optical path-length of a roundtrip is a multiple of the effective wavelength, constructive interference occurs and light is built up inside the ring. The length between the Ring and the straight guide was varied resulting to a varied power coupled in the Ring as shown in Fig 6.

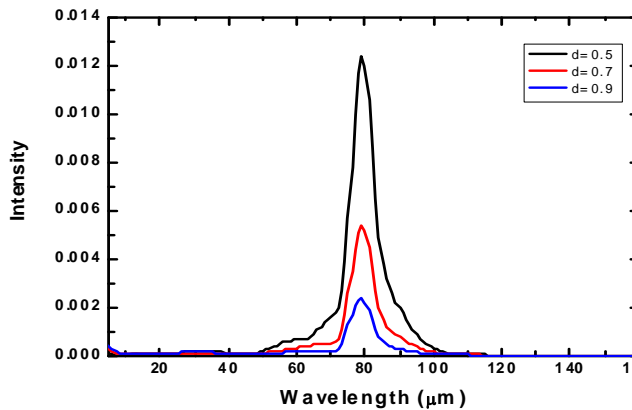


Fig 6: Comparison of power coupled in the ring on varying length

3.2 Variation of the length between the waveguide and the ring

A continuous source frequency $f=0.15$ PHz placed at point (-7, 3.8) in the lower waveguide. For this broadband source the resonance frequency was found to be in the range 0.068 GHz – 5.026 GHz. When length between the ring and the straight guide was increased by a small margin of $0.5 \mu\text{m}$ from an initial $0.5 \mu\text{m}$ interspace, there is an upward shift in the power that goes through the ring at points $54 \mu\text{m}$ and $104 \mu\text{m}$. In this case as the length is increased the filter characteristics of the optical band pass resonator fades away. This is shown in Fig 7.

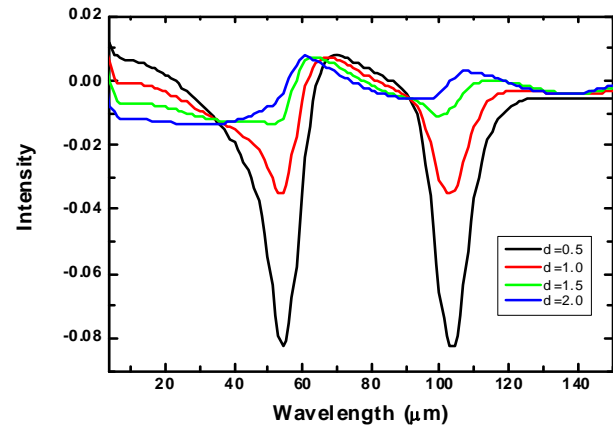


Fig 7: Variations in length between the ring and the straight guide

3.3 Variation of the computation cell

The physical parameters were $n=3.4$, $r=2.8 \mu\text{m}$, pulse frequency 0.15, PML= $1.0 \mu\text{m}$ and $w=1.0 \mu\text{m}$. The run time was set at 200. The results gave a shift in the wavelength with a decrease in the output power. This is the power that is coupled in the ring. In this a case a tunable [5] [10] filter was achieved.

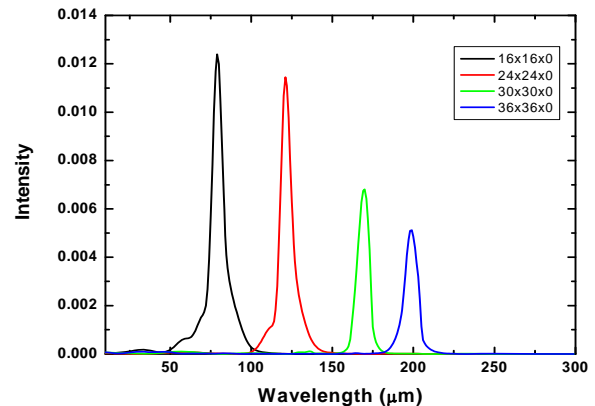


Fig 8: different computation cells showing a shift in a tunable filter

3.4 Power variation in different types of Rings



Fig 9: (a) single ring (b) double ring (c) triple ring

The shifting in the wavelength also arose when the structure of the ring was modified. First it was a ring and a single

waveguide, second was a ring and two straight waveguides, third was two rings and two straight waveguides and lastly three rings and two waveguides. As the rings were increased the power coupled during resonance kept on reducing. The outcome is as shown in Fig 10 and Fig 11.

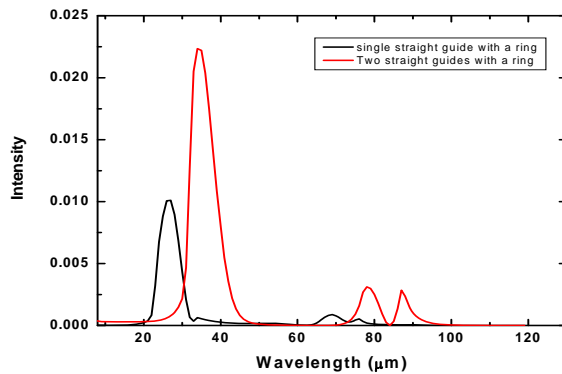


Fig 10: Single and double rings at resonance

For three rings and two waveguides

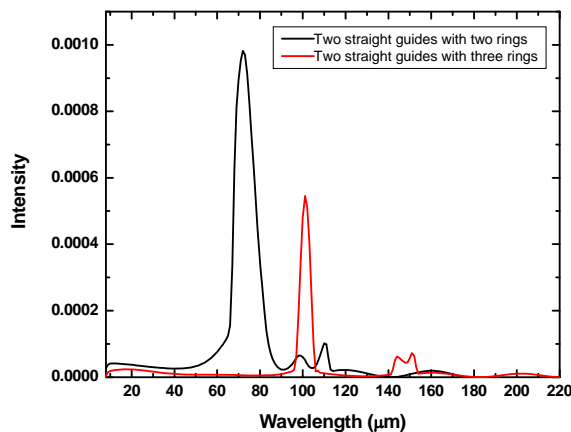


Fig 11: double and triple rings at resonance

IV. CONCLUSION

Explanation of using ring resonators for optical filtering in WDM was presented. The validation of analytical analysis using MEEP was carried out in this paper. Ring resonators allow for compact channel filters in WDM and represent a key component in modern optical networks. It was shown that tunable filter represent a good candidate for add/drop in WDM which will improve the selection of the optical signal and data fibre to home (FTH).

ACKNOWLEDGEMENT

The authors of this paper acknowledge the developers of the MEEP code and the University of Eldoret for the use of their

resources during this study, the fibre optic group and the entire physics group at university of Eldoret.

REFERENCES

- [1] Franchimon, E. (2010). Modelling circular optical microresonators using whispering gallery modes.
- [2] Ksendzov, A., & Lin, Y. (2005). Integrated optics ring-resonator sensors for protein detection. *Optics letters*, vol. 30, no. 24, pp. 3344-3346.
- [3] Miller, N. Microring Resonator Channel Dropping Filters.
- [4] Agarwal, A., Toliver, P., Menendez, R., Etemad, S., Jackel, J., Young, J., & Delfyett, P. J. (2006). Fully programmable ring-resonator-based integrated photonic circuit for phase coherent applications. *Journal of lightwave technology*, vol. 24, no. 1, p. 77.
- [5] Loh, P. R., Oskooi, A. F., Ibanescu, M., Skorobogatiy, M., & Johnson, S. G. (2009). Fundamental relation between phase and group velocity, and application to the failure of perfectly matched layers in backward-wave structures. *Physical Review E*, vol. 79, no. 6, p. 065601.
- [6] Hopkins, R. (2006, October). Influence of radiation losses in microstrip ring resonators used for materials characterisation. In *IMAPS 39th Int. Symp. Microelectronics* pp. 65-71.
- [7] Little, B. E., Chu, S. T., Haus, H. A., Foresi, J., & Laine, J. P. (1997). Microring resonator channel dropping filters. *Lightwave Technology, Journal of*, vol. 15, no. 6, pp. 998-1005.
- [8] Akleman, F., & Sevgi, L. (2008). Comparison of rectangular and cylindrical FDTD representations on a ring resonator problem. *Turkish Journal of Electrical Engineering & Computer Sciences*, vol. 16, no. 1, pp. 87-94.
- [9] Qiang, Z., Zhou, W., & Soref, R. A. (2007). Optical add-drop filters based on photonic crystal ring resonators. *Optics express*, vol. 15, no. 4, pp. 1823-1831.
- [10] Dong, P., Qian, W., Liang, H., Shafiqi, R., Feng, N. N., Feng, D., & Asghari, M. (2010). Low power and compact reconfigurable multiplexing devices based on silicon microring resonators. *Optics express*, vol. 18, no. 10, pp. 9852-9858.
- [11] Nawrocka, M. S., Liu, T., Wang, X., & Panepucci, R. R. (2006). Tunable silicon microring resonator with wide free spectral range. *Applied physics letters*, vol. 89, no. 7, p. 71110.
- [12] Yariv, A. (2000). Universal relations for coupling of optical power between microresonators and dielectric waveguides. *Electronics letters*, vol. 36, no. 4, pp. 321-322.
- [13] Yariv, A. (2002). Critical coupling and its control in optical waveguide-ring resonator systems. *IEEE Photonics Technology Letters*, vol. 14, no. 4, pp. 483-485.
- [14] Choi, J. M., Lee, R. K., & Yariv, A. (2001). Control of critical coupling in a ring resonator-fiber configuration: application to wavelength-selective switching, modulation, amplification, and oscillation. *Optics Letters*, vol. 26, no. 16, pp. 1236-1238.